Invited Talk

On Acoustic Emission Sensor Characterization

Kanji Ono
Department of Materials Science and Engineering, University of California, Los Angeles (UCLA),
Los Angeles, CA 90095, United States

ABSTRACT: We examined calibration methods for acoustic emission (AE) sensors. In spite of the self-evident needs of reliable calibration, the current state is deplorable globally. The only primary standard at NIST (US) is non-operational, yet no other standard has emerged. Widely practiced face-to-face calibration methods have no validated foundation. Reciprocity calibration methods are invalid for the lack of reciprocity and sensor dependent reciprocity parameters. This work provides three workable solutions based on laser-based displacement measurement, which leads to "direct" method using the face-to-face arrangement. This leads to the second "indirect" method of mutually consistent determination of transmitting and receiving sensitivities of sensors/transducers. For all ultrasonic and AE sensors examined, their receiving and transmitting sensitivities are found to be always different and non-reciprocal. Displacement vs. velocity calibration terminology is clarified, correlating the "V/μbar" reference to laser-based calibration. We demonstrate the validity of the direct and indirect methods and the third one based on Hill-Adams equation, called Tri-Transducer method. This uses three transducers as in reciprocity method, but incorporates experimentally determined reference sensor sensitivities ratio without a transfer block and can get both transmitting and receiving sensitivities. These three methods provide consistent calibration results for over 30 AE sensors.

1. INTRODUCTION

In acoustic emission (AE) testing, sensors are essential components of a nondestructive test system. Their characterization attracted much interest over the years. Notable reviews on AE sensor calibration appeared in the 1980s [1-3], but only established standards are two ASTM standards for the primary and secondary calibration of AE sensors [4, 5]. These are based on seismic pulse on a large transfer block, developed at NIST [6] and are for the calibration of the surface wave sensitivity. Currently, they are dormant. Burks and Hamstad [7, 8] reexamined the NIST procedures and suggested revisions. One of them is to use measured displacement, rather than analytical calculation since the capillary-break source is elliptical, rather than a point. No ASTM standard exists for AE sensor calibration for normal incidence waves.

AE sensor manufacturers typically provide a sensitivity curve based on face-to-face calibration. This calibration procedure has been treated as proprietary information and described only inadequately [9]. Calibration curves are usually in reference to the reference level of 1 V/μbar, but this reference remains undefined. ASTM E976 standard guide [10] is often cited as the basis, but E976 specifically excludes the face-to-face procedure. This widely practiced face-to-face calibration methods presently have no validated foundation. It does benefit from the ease of set-up, reasonably good repeatability and the ability to handle long-duration signals of high-sensitivity (undamped or minimally damped) AE sensors. Commonly used AE sensors reverberate beyond 1 ms when free and often over 200 μs even coupled to a metal block, enlarging the needed size of a transfer block to inconvenient sizes of over 1 m. Thus, it is desirable to give it physics-based validation.

Reciprocity calibration methods have been well established for acoustic transducers and hydrophones. In ultrasonic transducer calibration, more advanced methods have appeared and the frequency range extended to 20 MHz routinely [11] and to 100 MHz in laboratory [12-16]. These include uses of direct measurement of particle velocity in water, time-delay spectroscopic methods, an optical multilayer hydrophone as reference and pulse-echo with a reflector. This is in sharp contrast to the unsatisfactory state of AE sensor calibration. In general cases of differing transmitting and receiving sensitivities, Hill and Adams [17] showed that the reciprocity calibration method requires the independently determined ratio of transmitting and receiving sensitivities of an auxiliary transducer. This condition of non-reciprocity prevails in all the piezoelectric transducers examined [18]. We also showed [18] that reciprocity parameters are sensor-pair dependent. Reciprocity calibration methods for AE sensors [19-23] are thus invalid for the lack of reciprocity for AE and UT transducers when used in contact with solid medium.

In well-damped transducers, laser techniques provided satisfactory results for surface displacement/velocity measurement as discussed extensively by [24]. In the present study, we will utilize laser interferometry as the basis for sensor/transducer characterization [25] and consider three sensor calibration methods.

Let us denote the transmission output of the i-th transducer due to an electrical pulse as $T_i = t_i \cdot V_i$, where t_i is the transmit transfer function and V_i is the FFT spectrum of the pulse input. Here, the transducer output is measured in displacement. Using a laser interferometer, we can experimentally determine T_i or t_i. Next, R_j is the receiving displacement sensitivity spectrum of the j-th transducer. That is, voltage output for a given displacement input on the face of the receiver. When transducer i is coupled face-to-face with transducer j, this constitutes a transmission-reception (T-R) test. We get its output E°_{ij} with the above notation (without separating the input spectrum) as

$$E^{\circ}_{ij} = T_i \cdot R_j = t_i \cdot V_i \cdot R_j \qquad (1)$$

Knowing T_i from laser interferometry, R_j can be obtained. Actual calculation relies on the spectral division procedure using FFT magnitude spectra of E°_{ij}, T_i and R_j. This is designated as "Direct" method. Using the direct method, we can obtain the R_j spectra for any sensors (which need not be transmitting) and transducers (capable of transmitting as well). This method also applies to sensors with integrated preamplifiers.

Using transducers as transmitters in combination with sensors of known R_j, we can also determine their transmitting sensitivities, T_i via the same equation (1). Combining a transducer needing T_i with the sensors R_j, we determine multiple spectra of E°_{ij} with T-R tests. By spectral division with known R_j, T_i is determined. To minimize the scatter expected, it is normal to obtain several spectra for a particular transducer's transmitting sensitivity and average them. This is "Indirect" method. This method can also utilize the transmitting sensitivity thus obtained for getting receiving sensitivity spectra of still other sensors. Again, multiple spectra are averaged to minimize the scatter. Consistency of the present calibration procedures can be verified through the reconstruction of T-R tests comparing T_i and R_j thus obtained with experimentally measured E°_{ij}. Good consistency was found. Results of the indirect method are also compared with those of direct method. As shown later, two methods produced good agreement as well.

Since AE sensors are always used in contact with solid medium, it is desirable to evaluate them using a transfer block. With the above notation (without separating the input pulse spectrum) plus the transfer function of the transfer medium X_{ij}, a T-R test for transducers i and j leads to

$$E_{ij} = T_i \cdot X_{ij} \cdot R_j = E^{\circ}_{ij} \cdot X_{ij} \qquad (1a)$$

The transfer function X_{ij} can be obtained from equations (1) and (1a); Face-to-face T-R experiment provides E°_{ij}, while E_{ij} in (1a) comes from a T-R test through a transfer block. This X_{ij} function is dependent on a particular pairing of transmitter and receiver, requiring subscripts. Generally, T-R tests are not reversible; $E_{ij} \neq E_{ji}$.

Hill and Adams [3, 17] analyzed generalized cases of reciprocity calibration, in which T_i and R_i of transducers differ and the law of reciprocity is no longer satisfied. Three-transducer set-up is used as in classic reciprocity calibration methods. One of the three (auxiliary transducer) is used as a reference needing both T_i and R_i functions, while another acts as a transmitter. The third is the target of calibration and can be receiving only. Here, transducer pairs of 1 and 2, 1 and 3, and 2 and 3 are selected and transducer 3 is the auxiliary transducer while 2 is the target transducer of calibration. We have

$$E_{12} = T_1 \cdot X_{12} \cdot R_2,\ E_{13} = T_1 \cdot X_{13} \cdot R_3, \text{ and } E_{32} = T_3 \cdot X_{32} \cdot R_2. \qquad (2)$$

Taking ratio of the first two equations, $E_{12} / E_{13} = (X_{12} \cdot R_2)/(X_{13} \cdot R_3)$, we get $R_2 = (E_{12} \cdot X_{13} \cdot R_3)/ (E_{13} \cdot X_{12})$, and the third one yields: $R_2 = E_{32} /(X_{32} \cdot T_3)$. Combining, we have for pairs coupled through the transfer block

$$R_2 = [(X_{13} \cdot E_{12} \cdot E_{32} / X_{12} \cdot X_{32} \cdot E_{13})\ (R_3 / T_3)]^{1/2}. \qquad (3)$$

There are six unknowns of T and R for transducers 1 to 3, but T_2 was unused and T_1 cancels out in getting equation (3). We can thus obtain R_2 by getting from experiment six E_{ij} values that provide three X_{ij} and the ratio R_3/T_3, determined separately from these six T-R experiments. Notice that no transducer reciprocity is required in the above derivation.

We deviate here from [17] by using the transmission parameters X_{ij}. In Hill-Adams analysis, X was defined as a unique function of the transfer medium, because X is based on the Green's function for point to point transmission. Because of diffraction effects, each transducer pair of finite sizes has a unique X_{ij}. Also the size of the transfer block

is a factor, as well as the receiver size. For some pairs, X_{13}/X_{12} can be treated as unity over a limited frequency range and only X_{32} is needed. When X_{13}/X_{12} is unity, equation (3) reduces to Hill-Adams equation [17], given as

$$R_2 = [(E_{12} \cdot E_{32}/X \cdot E_{13})\,(R_3/T_3)]^{1/2}. \quad (3a)$$

Reciprocity calibration cannot provide the ratio of T_i and R_i of the reference transducer, required in equation (3) or (3a) expressing the receiving sensitivity, R_2. This problem can be overcome when T_i sensitivities are obtained using the laser interferometry, which in turn provide R_i sensitivities using the direct and indirect methods discussed above.

It is noticed that $E_{ij} = E^{\circ}_{ij} \cdot X_{ij}$ from equation (1a). Upon substitution into equation (3), we obtain

$$R_2 = [(E^{\circ}_{12} \cdot E^{\circ}_{32}/E^{\circ}_{13})\,(R_3/T_3)]^{1/2}. \quad (3b)$$

This means that X_{ij} and the use of transfer block are not required. Face-to-face arrangement can replace calibration procedures with a transfer block. We designate this approach without a transfer block based on equation (3b) as Tri-Transducer (TT) method.

We examine here the inadequacy of sensitivity calibration methods for AE sensors available today and provide three workable solutions based on physically measureable quantities. Other related issues are also discussed including front-loading effects and μbar reference.

2. TRANSDUCER SENSITIVITY CALIBRATION – TRANSMISSION AND RECEPTION

The use of laser interferometry for transducer calibration is straightforward [24, 25]. Commercial interferometers of various design are now available, although their uses have been limited due to high cost. Two works [21, 22] made significant advances using laser interferometry to verify the displacement of surface pulse and obtained the sensitivity for surface-wave reception of PAC μ-80 and UT1000 sensors. This approach is a good supplement to the NIST method.

In our studies that have focused on normal incident waves, we have used a displacement-sensitive laser interferometer (Thales, LH140, 20 MHz bandwidth with the sensitivity of 0.1 V/nm at Aoyama Gakuin University, Sagamihara, Japan; Dr. H. Cho graciously conducted measurement). Three typical transmission curves with a fast initial rise and slower decay with several oscillations are shown for broadband ultrasonic transducers (Olympus V101, V103 and V104) in Fig. 1a with their corresponding FFT magnitude in dB scale (Fig. 1b). The peak displacement values are 10 - 12 nm. These are shifted in time and level as noted. The raw FFT spectral data contained noise and it was reduced by using 25-point smoothing Savitzky-Golay algorithm [26]. The observed displacement waveforms are basically of mono-polar shape with trailing oscillations. This feature results from the forward radiation at the front face and the presence of absorber behind piezoelectric element, as predicted by theory [27, 28]. The peak displacement value is approximately 50 pm/V, which is expected from a typical lead-metaniobate piezoelectric element. The other half of piezoelectric displacement is radiated backward into the absorber and mostly damped.

The FFT magnitude transmitting spectrum is relatively smooth for V104 (Fig. 1b). The spectra of V101 and V103 shows many peaks and dips, showing strong fluctuation. Some of them are extraneous vibrations as the transducer front face is free, only facing air. With face-to-face arrangements, these apparently disappear as these transducers produced smooth spectral curves in T-R tests. Front-face loading effectively suppressed extraneous vibrations. It appears that the low frequency oscillations coming from radial resonance are not suppressed adequately. Comparing six T_i spectral curves, we selected to use V104 as the reference transducer and use the remaining five for confirmation by avoiding the range where irregular changes are observed.

The transmission characteristics of V104 are shown in Fig. 2 up to 5 MHz, though higher range is less important in AE. The HV pulse spectrum is curve 1. The displacement transmitting spectra of V104 are curves 2 and 4 (unit = nm). The latter is corrected by subtracting the HV FFT spectrum, indicating much less frequency dependence of V104 transmission and showing a broad peak at 2.6 MHz. By multiplying the angular frequency, $2\pi f$, these curves are converted to show the velocity response of V104 transmission, curves 3 and 5 (unit = m/s), with or without the HV electrical pulse spectrum.

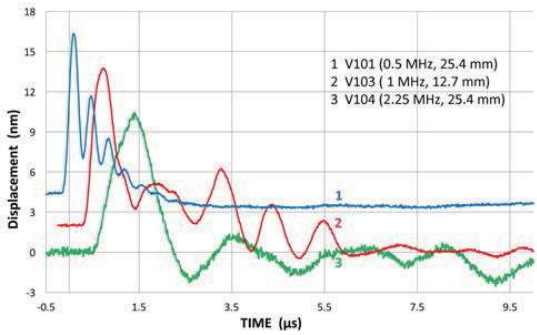

Fig. 1 a. Displacement waveforms of three transducers.

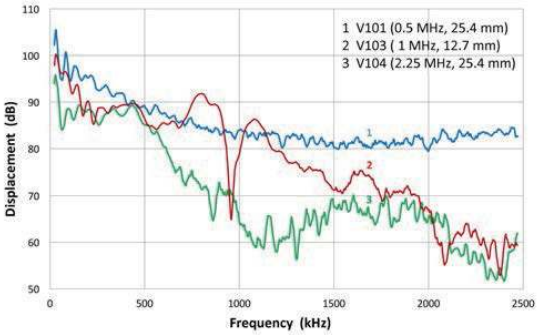

b. FFT displacement spectra, re. 0 dB at 1 nm.

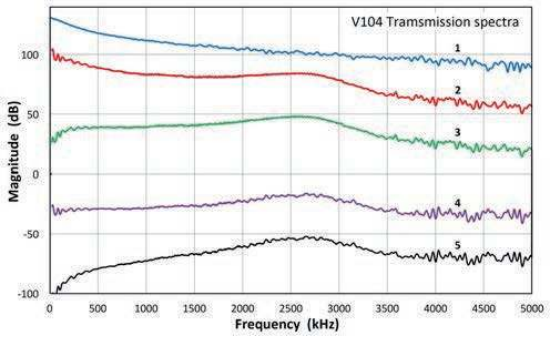

Once T_{V104} of the reference transducer is obtained, we determine R_i of other transducers by conducting T-R test in a face-to-face arrangement of the reference against a sensor under test (SUT) using equation (1). This provides E° for the transducer-sensor pair. The R_{SUT} is then determined by $R_{SUT} = E^\circ - T_{V104}$. The 0 dB reference for the R_{SUT} is 1 V/nm with frequency in kHz.

Fig. 2 Transmission spectra of V104. 1. HV pulse only, 2. Displacement (nm), 3. Velocity (m/s), 4. 2 less HV pulse (nm/V), 5. 3 less HV pulse ((m/s)/V).

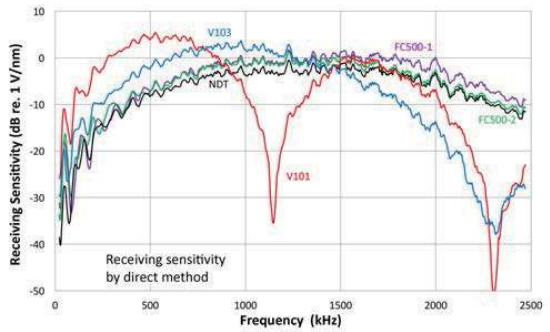

Fig. 3 Receiving sensitivities of 5 UT transducers.

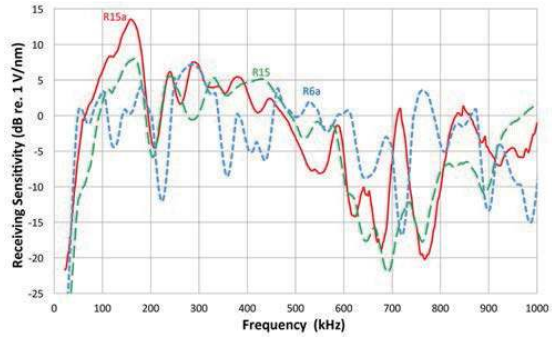

Fig. 4 Receiving sensitivities of 3 AE sensors.

Using V104 transmitter, we first examine the response of a conical PZT sensor, home-made using the Proctor design [29]. The conical FFT spectrum minus T_{V104} spectrum has broad distribution, reaching the maximum at -15 dB, in good agreement with the value of -14 dB Proctor reported for his conical sensors [29]. Next, using the direct method and five UT transducers, all well damped, we obtain the R_{SUT} curves (Fig. 3). Three 2.25 MHz transducers show similar smoothly varying sensitivities except V101 and V103 have major dips at 1.1 and 2.3 MHz. These all show the peak of -2 to +5 dB sensitivity and large fluctuations at low frequencies.

The direct method used for broadband UT transducers applies to general-use AE sensors as well. These are typically of higher sensitivity and most have more than a single resonance. Three receiving spectra are shown in Fig. 4. PAC R15a is most sensitive here, showing a peak displacement sensitivity of 13 dB at 162 kHz. PAC R15 shows a similar spectral shape, but shows a little lower sensitivity. PAC R6a is a newer sensor, but this is designed for low frequency (60 kHz) surface-wave detection: here the peak is near 300 kHz. All of these general-use AE sensors have the peak sensitivity of 0 to 13 dB or about 1 to 4.5 V/nm.

Next, we used nine UT transducers as transmitters and receivers. By using multiple T_i and R_i sensitivity spectra thus obtained, the T_i and R_i sensitivity spectra of any transducer can be determined. This is the “Indirect” method. In order to get T_i of transducer A, couple it to transducers B, C, D, etc. with known R_i spectra. Since results vary

slightly, they are averaged to finalize the T_A sensitivity of transducer A. Even though the laser-based T_i sensitivities showed some irregular peaks and dips, the averaged spectra are generally smooth, indicating the front-face loaded T_i sensitivities have smooth spectra. An example of the T_i sensitivity of NDT thus obtained is shown in Fig. 5 and compared to that due to laser interferometry. These two curves differ by 0.7 dB on average over 22-1400 kHz. For the indirect spectra, the absence of two large dips at 1.5-2 MHz indicates that the front-face loading removed extraneous vibration through the coupling of a receiving sensor. In the present case, both front face materials are alumina plates with matching acoustic impedance. The indirect method can be applied in reverse to determine the R_i spectra of a transducer. Three such examples are shown in Fig. 6. These have the peak sensitivity of about 1 V/nm. Results of the two methods, direct and indirect, generally agree better than 0.5 dB on average to 2 MHz. Maximum difference reaches 5 dB at low frequencies.

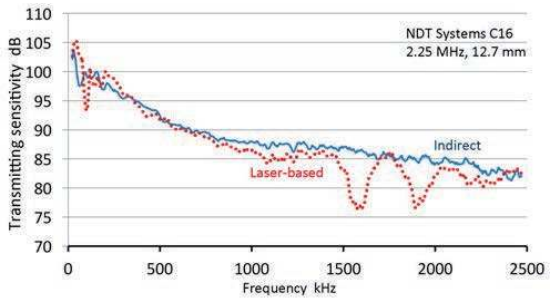

Fig. 5 T_{NDT} by laser-based and indirect methods.

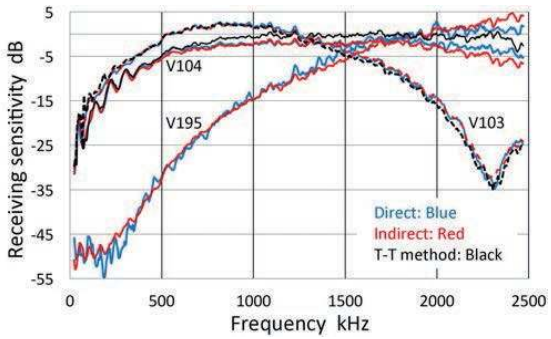

Fig. 6 R_i spectra of 3 transducers by various methods.

Finding both T_i and R_i spectra of a transducer, we can verify these calibration results. This is done by constructing the combined T_i and R_j ($i \neq j$) spectrum for any combination of transducers and comparing it with the corresponding T-R experiment. An example is given in Fig. 7, where V189 and V195 were paired. T_{V195} spectrum was obtained from other transducers' R_j spectra and is marked V195 T (red). R_{V189} is the bottom curve. The sum of these two is plotted as T + R in purple and is compared to face-to-face output, marked T R (exp) in green curve. These two agree well over 150-1200 kHz and 1.3-1.7 MHz, but poorer near the dip of R_{V189} and above 1.7 MHz. For twelve cases examined in detail, spectral comparison yielded better than this example. The average discrepancy was typically about 1 dB except below 200 kHz or above 2 MHz, where discrepancy is slightly higher. For validation purpose, we can also utilize laser-based transmitting sensitivity (but avoiding the frequency range that shows irregular peaks and dips: >250 kHz for V101, >650 kHz for V103, >1400 kHz for NDT C16). These were set aside in preference of using V104, but they do provide a back-up. Here, agreement was moderate.

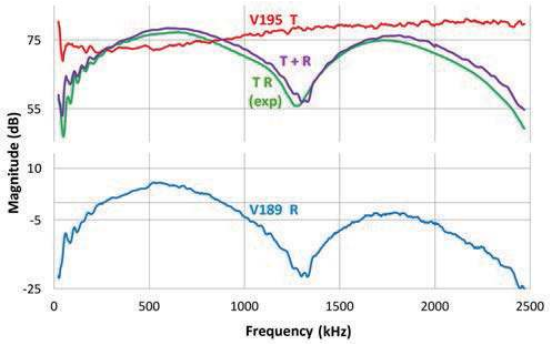

Fig. 7 Combined T_{V195} + R_{V189} vs. TR test spectrum.

In the above comparative procedure of the combined T_i and R_j sensitivity versus directly measured T+R sensitivity, it is necessary to account for the area of a receiving sensor when it is larger than the transmitter it is paired with. Assuming that the receiving sensitivity is uniform over the entire area, one adds 4.99, 7.04 and 12.04 dB for the diameter ratio of 1.333, 1.5 and 2, respectively. The present results of good matching of the experimental combined spectrum and one deduced from the calibration of T_i and R_j spectra indicate the uniformity assumption is valid. We can thus determine mutually consistent transmitting and receiving sensitivities of transducers and sensors.

The ratios of the R_i sensitivity and t_i sensitivity (excluding the HV pulse spectrum) were obtained for 17 transducers including both broadband and resonance types. Surprisingly, the general spectral shapes of R_i/t_i spectra were similar except for shift in values. Four examples are shown in Fig, 8. Below about 600 kHz, the spectral difference exhibits the dependence is $f^{1.8}$ for V101, and $f^{1.33}$ for the rest. All show a peak around 800 kHz and start decreasing at higher frequencies. It is also strange that the middle two curves for V103 and V104 are essentially identical despite their non-matching sensitivity spectra. All other curves are between the top and bottom (except V195). This observation on R_i/t_i -ratios can be related to the spectral difference between a half-sine mono-polar

displacement pulse and a full-cycle sinewave pulse (approximating a Gaussian pulse and its derivative). The difference of their FFT spectra is also plotted in Fig. 8 as a blue (dash-dot) curve. The lower frequency part is linear with frequency until it approaches the peak at 900 kHz. The transmission pulse shapes from damped transducers are usually mono-polar, just like a half-cycle sinewave (see Fig. 1a). In contrast, the received signals tend to have an oscillatory, bi-polar shape. The differing transmission and reception behaviors originate from the mechanisms of pulse generation of a piezoelectric element [27] and produce the observed spectral ratio.

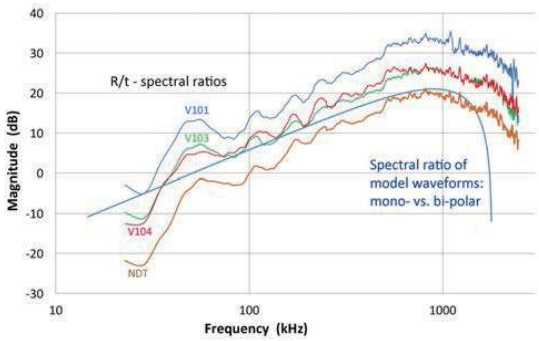

Fig. 8 Spectral ratios of transducers and model waves.

This section demonstrates that 1) the direct method of calibration is successfully used with the face-to-face arrangement, providing receiving sensitivity of various sensors/transducers, 2) the indirect method is used to determine both transmitting sensitivity and receiving sensitivity, 3) the indirect method suppressed extraneous oscillations of transmitters that may occur in free space, 4) calibration results of the two methods agree well, 5) mutual consistency of transmitting and receiving sensitivities is verified and 6) the receiving and transmitting sensitivities of a transducer always differ while their ratio shows similarity among various transducers.

3. VELOCITY RESPONSE OF A TRANSDUCER

We have shown that piezoelectric sensors generate output voltages responding to displacement input. It can still be described in terms of the time-derivative of displacement input, namely, particle velocity. The standard approach started with ASTM E1106 [4], which treats a sensor output to be proportional to the displacement function with a typical unit of V/nm. However, its FFT magnitude can be converted to express the sensitivity in reference to the input velocity function. This is accomplished by the multiplication of $2\pi f$ factor to the input function according to an identity in Fourier transform theory. When one divides the sensor output function by the velocity input function, the velocity sensitivity spectrum is obtained with a typical unit of V/m/s or Vs/m. The T_i spectra in terms of displacement can be treated in this manner, as shown in Fig. 5, curve 3. Here, the unit was changed from nm to m, corresponding to 180 dB subtraction in dB-scale. A note of caution: one cannot multiply $2\pi f$ to a receiving displacement sensitivity spectrum in an attempt to get the velocity response. Instead, you need an opposite operation: Divide by $2\pi f$ and add a factor of 10^{+9}.

In the AE field, it is common to find the use of μbar in place of m/s as the unit of velocity. This originated from Dunegan's use in 1968 of hydrophone calibration scheme in characterizing a reference transducer [30]. In 1968, Dunegan obtained calibration up to 400 kHz. Today, the frequency limit for miniature ultrasonic hydrophone calibration is extended to 20 MHz [11]. The physical meaning of 1 μbar reference pressure has not been articulated in any AE standard documents. When an AE sensor receives the pressure wave, most of the wave is reflected back into water as the the acoustic impedance of the sensor facing or sensing element is usually much higher than that of water. The transmitted pressure wave generates particle velocity in the sensor facing or the sensing element. However, this pressure cannot be measured. Thus, it is impractical to use it as the basis for calibration. In a recent study, Burks and Hamstad [9] concluded that the conversion procedure of sensor response to V/μbar reference is illogical and arbitrary unless one measures "the transient output pressure as a function of frequency from the driving transducer".

The most logical interpretation of V/μbar reference is that of pressure in water, as practiced in the underwater acoustics field for the hydrophone calibration [31]. In the immersion tank where a hydrophone is calibrated, the acoustic pressure field is known as a function of frequency. The acoustic pressure in water is defined as the product of the acoustic impedance of water (1.48 MPa/(m/s)) and particle velocity. Thus, the pressure of 1 μbar (= 0.1 Pa) in water corresponds to 67.6 nm/s. By placing a reference transducer at the position of known acoustic pressure, it can be calibrated as a function of frequency. This can then be combined with a broadband transmitter in face-to-face arrangement, from which the transmitter output can be calibrated in reference to equivalent acoustic pressure with the unit of μbar. Subsequently, a sensor under test is substituted for the reference transducer and calibrated in terms of V/μbar reference. With this interpretation, the commonly used reference of AE sensors, 1 V/μbar, can be related to physically based reference of 1 V s /m. That is, 0 dB (ref. 1 V/μbar) is 143.4 dB in reference to 0 dB at 1 V s/m. Alternately, xx dB in ref. to 1 V s/m = xx – 143.4 dB in ref. to 1 V/μbar.

Some R_i sensitivity curves for common AE sensors are shown in Fig. 4. These have the peak sensitivity of around 0~15 dB in reference to 0 dB at 1 V/nm. After converting their response to volts per unit velocity of 1 m/s, we have the velocity response curves for one of them (R15a) shown in Fig. 9. Curves plotted on the lower side are further converted in reference to the scale of 0 dB at 1 V/μbar. For PAC R15a, the calibration provided by the manufacturer is plotted as green curve, just above the lower velocity spectrum. Their values are typically 10-20 dB above our calibration for >0.1 MHz and the shape of this curve matches better with the displacement calibration. This discrepancy exists for almost all other sensors examined, not just from this manufacturer, implying a possible existence of industry-wide systematic error. An interim solution is to add 72-74 dB to manufacturer's calibration, thereby obtaining the displacement calibration in reference to 0 dB at 1 V/nm.

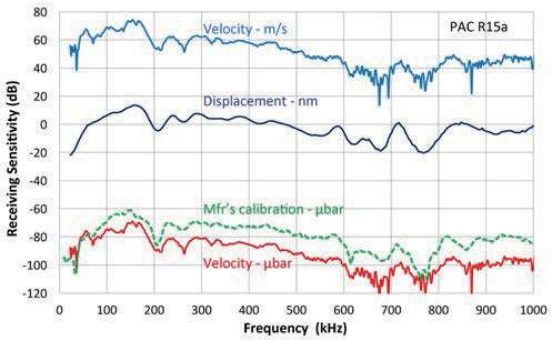

Fig. 9 Velocity calibration curves of R15a sensor.

It is worthwhile to consider direct differentiation of displacement waveforms from transmitters to velocity waveforms. This procedure uses the Savitzky-Golay algorithm [26] and offers physical insight to velocity output. The waveform changes from monopolar to bipolar and the rise time was halved. As expected, the FFT spectra are comparable with the $2\pi f$-multiplication curves. The above discussion shows that it is unproductive to classify a sensor to displacement-response or velocity-response without specifying the frequency range or the flatness of response. NIST-type conical sensors with a large mass backing clearly have a broad range of flat displacement response, while typical accelerometers are designed to produce nearly flat wideband response in acceleration below the resonance frequency. Common AE sensors have been designed for resonance-based peak sensitivity, while newer designs start to broaden the peak sensitivity ranges.

This section leads to the clarification of pressure calibration references in terms of 1 V/(m/s) and 1 V/μbar and demonstration of equivalence of two conversion methods to velocity.

4. RECIPROCITY AND TRI-TRANSDUCER CALIBRATION METHODS

Our laser-based calibration method has demonstrated that the T_i and R_i sensitivities of UT and AE transducers differ. Hill and Adams [17] analyzed the classic reciprocity methods for the cases appropriate for contact piezoelectric transducers. In their analysis of reciprocity calibration methods, T_i and R_i sensitivities are not required to be identical; that is, non-reciprocal. This exactly fits the experimental reality we have established. Their analysis led to the receiving sensitivity of sensor 2, R_2, to be given by Hill-Adams equation (3a) for pairs coupled through the transfer block, where X is the point-wise transfer function of the propagating medium. This result leads to the demise of reciprocity calibration methods for piezoelectric contact transducers since there are six unknowns and only three equations. You cannot also express T_i sensitivity from E_{ij} and X. Thus, without transducer reciprocity, current reciprocity calibration methods lack the foundation [19-23].

We have obtained T_i, R_j and R_j/T_j spectra for over 25 transducers. The ratio, R_3/T_3, needed in Hill and Adams equation, is frequency dependent, increasing with frequency, as shown in Fig. 10. Some are similar, but usually the spectra match poorly. Another parameter needed in Hill and Adams equation is X, which corresponds to the attenuation of longitudinal wave as it passes the transfer block. Experimentally, we find this to be dependent on a particular pair of transducers. A few examples are shown in Fig. 11. In our testing, a transfer block was of Al 7075 alloy (300 x 300 x 156 mm) with waves traveling normal to the broad faces. While X_{ij} between two UT transducers is relatively smooth, those including a resonant sensor (R15) have large fluctuations. Diffraction effects and sensor resonances contribute to the prominent features. Overall trend is consistent, however. Deriving X_{ij} functions from point-wise transfer function is a complex task, especially when one must also include resonance effects. Now, this is a moot point as X_{ij} parameters have canceled out in equation (3b) and are no longer required in the Tri-Transducer (TT) method.

Before realizing that equation (3) reduces to (3b), eliminating the need of X_{ij} parameters, we evaluated R_i for 20 combinations using the extended Hill-Adams equation (3). These results are identical to those using equation (3b), or TT method. Fig. 12 shows the case for 1) 1 MHz UT, 2) FC500-2 and 3) FC500-1. The spectra for three E_{ij} (top group), R_2 (FC500-2) and the same from laser method (middle), and R_3/T_3 for FC500-1 (bottom curve) are plotted.

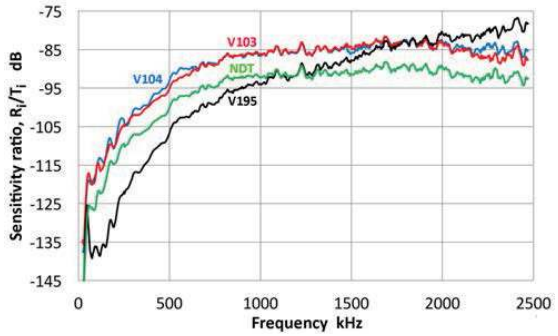

Fig. 10 Spectral ratio, R_i/T_i, for four transducers.

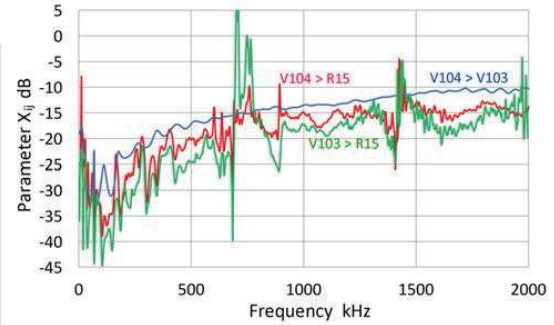

Fig. 11 Parameter X_{ij} for V104, R15 and V103.

The values of R_2 by the TT and direct methods agree quite well below 1.5 MHz with the average difference of 0.34 dB. The dip in the two E_{ij} curves are from #1, but it has no effect on the outcome. Even when two resonant sensors are in the group of 3 (not shown), the values of R_2 for R15a by the two methods are close, with the average difference of 1 dB below 600 kHz. Considering many peaks and dips in the spectra, this is a good match. These two cases show that the choice of transducer 1 is non-critical: just needed to transmit in the frequency range of interest. However, size correction is needed when receiver (SUT) is larger than the other two or reference transducer 3 is larger than the transmit-only transducer 1. Two more results of the TT method are given in Fig. 6. Two transducers, V103 and V104, show good to excellent agreement with the direct and indirect methods. With V103, average differences between the three methods to 2 MHz were 0.06, 0.25 and 0.19 dB. V104 results gave slightly higher average differences of 0.32, 1.36 and 1.04 dB. These values are for a set of experiment. By averaging, multiple set testing should further improve the performance. It is also necessary to explore the sources of errors.

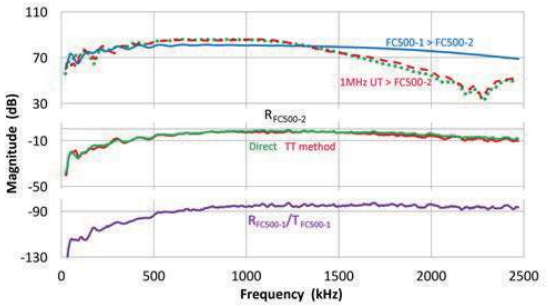

Fig. 12 Spectra for $R_{FC500-2}$ with a tri-transducer test.

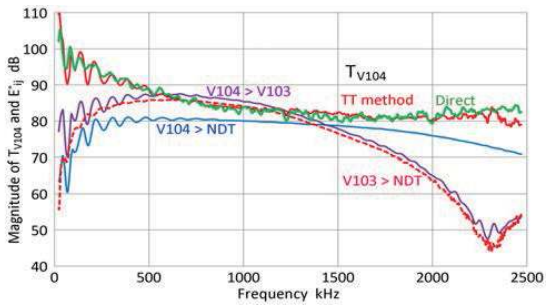

Fig. 13 T_{V104} by direct (laser) and TT methods.

This Tri-Transducer method developed from Hill-Adams analysis is beneficial for its reliance on the sensitivity ratio and avoiding direct use of displacement transmission reference alone. Reception from another transmitter is included so we can avoid potential problems that may arise from a particular combination of transducers. Still, this approach does require the determination of R_3/T_3 ratio of reference transducer 3 by laser interferometry. The TT-method has been used for over 20 combinations of three-transducers. Average difference (over 22 kHz to 2 MHz) with the result of direct method is typically less than 0.5 dB, although a few cases show values of 1 to 2 dB.

The TT method can be used to obtain the transmitting sensitivity, T_1, similarly to the indirect method. We have

$$T_1 = [(E^\circ_{12} \cdot E^\circ_{13}/E^\circ_{32})\,(T_3 / R_3)]^{1/2}. \qquad (4)$$

An example is plotted in Fig. 13. Three transducers used are V104, NDT and V103. Each of E°_{ij} curves peaks at 0.5-1 MHz. The transmitting spectra for V104 are obtained using the TT method with equation (4) (red) and compared to the result of the direct method (green). Except for oscillations below 200 kHz or above 2.3 MHz, excellent agreement is seen. The average difference in T_{V104} was 0.12 dB over 22 kHz to 2 MHz. Three additional TT tests (including PAC Pico and S9220) produced comparable T_{V104}. The averaged T_{V104} spectrum with the TT method differed from the direct method by 0.42 dB in the frequency range to 2 MHz. In addition, three T_{V103} spectra with the TT method agreed better than 0.2 dB with that from the indirect method. With this method for getting T_i, the use of some resonant sensors as a receiver produced poor results and should be avoided. This approach provides a new means of verifying the laser interferometry and the front loading effects.

Conclusions from this section are:

1) With demonstrated differences in the transmitting and receiving sensitivities of UT and AE transducers, current reciprocity calibration methods for AE sensors is invalid. Experimentally obtained longitudinal wave reciprocity parameter X varies depending on transducer pair used and not invariant as the reciprocity theory requires.

2) Equation (3) derived by extending Hill and Adams equation reduces to equation (3b). Needs for X parameter vanished, but physically measured ratio of R_3/T_3 is still required for Tri-Transducer method.

3) Tri-Transducer method is tested for over 20 combinations and shows good to excellent agreement with those from direct or indirect methods. This provides both transmitting and receiving sensitivities.

5. CONCLUSIONS

We examined outstanding issues of sensitivity calibration methods for ultrasonic and acoustic emission transducers. Determining spectral sensing properties is of utmost importance, especially in AE sensors, but recent research activities in this area have been low. In addition, today's emphasis in this field has been to model the sensor behavior using lumped parameter approach so that it can be integrated into systems modeling. On the other hand, physics-based analysis of piezoelectric sensing has been limited until recently. With new tools available today, laser interferometers and advance modeling methods, we are closer to the goal of finding a suitable and workable approach to transducer calibration and clarifying underlying sensing mechanisms.

Laser-based displacement measurement leads to the determination of transmitting sensitivities of transducers. This is Direct method. While simple in concept, some transducers generate extraneous vibrations on the front surface when it is free from solid contact. This issue was overcome by a suitable selection of a transmitter and by using an indirect method through the use of receiving sensitivities of other transducers. It was then possible to obtain mutually consistent transmitting and receiving sensitivities. This is Indirect method. The results also establish the foundation for face-to-face calibration methods, which were beset by the uncertainty of input parameters without access to the transmitter face. Good to excellent agreement has been observed between results of the direct and indirect methods using 30 sensors. Further, it is discovered that the receiving and transmitting sensitivities of over 20 transducers are always different, while their ratios exhibit unexpected similarity. The latter characteristics is traced to mono-polar pulse generation of damped piezoelectric transducers as a transmitter and, as a receiver, bi-polar received signals due to the reflection on the back face. This occurs even in transducers with good backing, likely from electrical impedance mismatch and charge transfer during elastic wave motion.

The observed difference in the receiving and transmitting sensitivities of a transducer leads to the invalidation of reciprocity calibration methods for piezoelectric contact transducers. The issue was raised in 1979 [17], but users of reciprocity calibration have ignored the fact that a separate measurement of ratio of the transmitting and receiving sensitivities is required. We have also measured the reciprocity parameters X in the case of through-transmission and found this to be dependent on transducer pairings, sizes, frequency, etc. in direct conflict with its definition in the reciprocity calibration methods. These are also not reversible in cases of different sized pairs.

After following Hill-Adams derivation, we found that parameters Xs cancel out, simplifying the expression for the receiving sensitivity, i.e., equation (3b). This is the basis for Tri-Transducer method, which has been tested for over 20 combinations. Results show good to excellent agreement with those from direct or indirect methods. The TT method can also provide the transmitting sensitivities of transducers, allowing a check of the laser method.

Displacement vs. velocity calibration terminology is examined, in view of ill-defined "V/μbar" reference used in commercial reporting of sensor property. Returning to the origin of its introduction by Dunegan [30], definition from hydrophone calibration standards clarified the reference. Procedure is given for converting between the velocity sensitivities in reference to unit velocity of 1 m/s and to acoustic pressure of 1 μbar.

ACKNOWLEDGMENT

The author wish to thank Dr. Hideo Cho of Aoyama Gakuin University, Sagamihara, Japan for running laser interferometer measurement. He also appreciates valuable discussion over many years with Dr. Al Beattie, Mr. Hal Dunegan, Prof. M.A. Hamstad, Dr. A.A. Pollack, Dr. Markus Sause as well as with his colleagues at UCLA, Profs. Ajit Mal and Vijay Gupta.

REFERENCES

[1] Sachse, W. and Hsu, N.N.; Ultrasonic transducers for materials testing and their characterizations, *Physical Acoustics*, 1979, 14, Academic Press, New York. pp. 277-406.

[2] Hsu, N.N.; Breckenridge, F.; Characterization of acoustic emission sensors. Mater. Eval., **1981**, 39, 60–68.

[3] Hill, R.; Reciprocity and Other AE Transducer Calibration Techniques, J. Acoust. Emiss., **1982**, 1, 73-80.

[4] ASTM E1106-12 Standard method for primary calibration of acoustic emission sensors, 2016, ASTM International, West Conshohocken, PA, USA, 12 p.

[5] ASTM E1781-13 Standard Practice for Secondary Calibration of Acoustic Emission Sensors, 2016, ASTM International, West Conshohocken, PA, USA, 7 p.

[6] Breckenridge, F.R.; Tscheigg, C.; Greenspan, M.; Acoustic emission; some applications of Lamb's Problem. J. Acoust. Soc. Am., **1975,** 57, 626–631.

[7] Burks, B.; Re-Examination of NIST Acoustic Emission Sensor Calibration: Part I - Modeling the loading from glass capillary fracture, J. Acoust. Emiss., **2011**, 29, 167-174.

[8] Hamstad, M.A.; Re-Examination of NIST Acoustic Emission Sensor Calibration: Part II - Finite element modeling of acoustic emission signal from glass capillary fracture, J. Acoust. Emiss., **2011**, 29, 175-183.

[9] Burks, B.; Hamstad, M.A.; An Experimental-numerical Investigation of the Face-to-face Sensor Characterization Technique, Mat. Eval., **2015**, 73, 414-423.

[10] ASTM E976-10 Standard Guide for Determining the Reproducibility of Acoustic Emission Sensor Response, 2016, ASTM International, West Conshohocken, PA, USA, 7 p.

[11] http://www.npl.co.uk/acoustics/underwater-acoustics/products-and-services/calibration-of-hydrophones-and-projectors Last updated on Mar. 25, 2010.

[12] Esward, T.J.; Robinson, S.P.; Extending the frequency range of the NPL primary standard laser inteferometer for hydrophone calibration to 60 MHz, IEEE Trans. Ultrason. Ferroelectr. Freq. Control, **1999**, 46(3), 737–744.

[13] Theobald, P.D.; Robinson, S.P.; Thompson, A.D.; Preston, R.C.; Lepper, P.A.; Wang, Y.; Technique for the calibration of hydrophones in the frequency range 10 to 600 kHz using a heterodyne interferometer and an acoustically compliant membrane, J. Acoust. Soc. Am., **2005**, 118, 3110-3116.

[14] Ludwig, G.; Brendel, K.; Calibration of hydrophones based on reciprocity and time delay spectrometry, IEEE Trans. Ultrason. Ferroelectr. Freq. Control, **1988**, 35(2), 168–174.

[15] Radulescu, E.G.; Lewin, P.A.; Wojcik, J.; Nowicki, A.; Calibration of ultrasonic hydrophone probes up to 100 MHz using time gating frequency analysis and finite amplitude waves, Ultrasonics, **2003**, 41, 247–254.

[16] Wilkins, V.; Koch, C.; Amplitude and phase calibration of hydrophones up to 70 MHz using broadband pulse excitation and an optical reference hydrophone, J. Acoust. Soc. Am., **2004**, 115, 2892-2903.

[17] Hill, R.; Adams, N. L.; Reinterpretation of the Reciprocity Theorem for the Calibration of Acoustic Emission Transducers Operating on a Solid, Acustica, **1979**, 43, 305-312.

[18] Ono, K.; Calibration Methods of Acoustic Emission Sensors, Materials, (submitted for publication), 2016.

[19] Hatano, H.; Watanabe, T.; Reciprocity calibration of acoustic emission transducers in Rayleigh-wave and longitudinal-wave sound fields. J. Acoust. Soc. Am., **1997**, 101, 1450–1455.

[20] NDIS-2109-91 Method for absolute calibration of acoustic emission transducers by reciprocity techniques, 1991, revised 2004, Japanese Soc. for Non-destructive Inspection, Tokyo, Japan.

[21] Goujon L.; Baboux J C.; Behaviour of acoustic emission sensors using broadband calibration techniques, Meas. Sci. Technol., **2003**, 14, 903–908.

[22] Keprt, J.; Benes, P.; A comparison of AE sensor calibration methods, *Proc. The 28th European Conf. on Acoustic Emission Testing*, 2008, Cracow Univ. Tech., Krakow, Poland. pp. 19-24.

[23] Monnier, T.; Dia, S.; Godin, N.; Zhang, F.; Primary Calibration of Acoustic Emission Sensors by the Method of Reciprocity, Theoretical and Experimental Considerations, J. Acoust. Emiss., **2012**, 30, 152-166.

[24] Scruby, C.; Drain, L.E.; *Laser Ultrasonics; Techniques and Applications*. 1990, Taylor & Francis, London.

[25] Ono, K.; Cho, H.; Matsuo, T.; Transfer functions of AE sensors, J. Acoust. Emiss., **2008**, 26, 72-90.

[26] Savitzky, A.; Golay, J.E.; Smoothing and Differentiation of Data by Simplified Least Squares Procedures, Analytical Chem., **1964**, 36, 1627-1639.

[27] Redwood, M.; Transient performance of a piezoelectric transducer, J. Acoust. Soc. Am., **1961**, 33(4); 327-334.

[28] Kossoff, G.; The Effects of Backing and Matching on the Performance of Piezoelectric Ceramic Transducers, IEEE Trans. Sonics and Ultrasonics, **1966**, SU-13, 20-30.

[29] Proctor, T.; An improved piezoelectric AE transducer, J. Acoust. Soc. Am., **1982**, 71, 1163–1168.

[30] Dunegan, H.L.; private communication, 2008.

[31] ANSI SI.20-1972, *Procedures for Calibration of Underwater Electroacoustic Transducers* and IEC 62127-2, *Ultrasonics-Hydrophones*.